

Evidence for a defect level above the conduction band edge of InAs/InAsSb type-II superlattices for applications in efficient infrared photodetectors

A. D. Prins, M. K. Lewis, Z. L. Bushell, S. J. Sweeney, S. Liu, and Y.-H. Zhang

Citation: [Applied Physics Letters](#) **106**, 171111 (2015); doi: 10.1063/1.4919549

View online: <http://dx.doi.org/10.1063/1.4919549>

View Table of Contents: <http://scitation.aip.org/content/aip/journal/apl/106/17?ver=pdfcov>

Published by the [AIP Publishing](#)

Articles you may be interested in

[Bias-selectable dual-band mid-/long-wavelength infrared photodetectors based on InAs/InAs_{1-x}Sb_x type-II superlattices](#)

Appl. Phys. Lett. **106**, 011104 (2015); 10.1063/1.4905565

[High performance photodiodes based on InAs/InAsSb type-II superlattices for very long wavelength infrared detection](#)

Appl. Phys. Lett. **104**, 251105 (2014); 10.1063/1.4884947

[Demonstration of high performance bias-selectable dual-band short-/mid-wavelength infrared photodetectors based on type-II InAs/GaSb/AlSb superlattices](#)


Appl. Phys. Lett. **102**, 011108 (2013); 10.1063/1.4773593

[Gallium free type II InAs/InAs_xSb_{1-x} superlattice photodetectors](#)

Appl. Phys. Lett. **101**, 071111 (2012); 10.1063/1.4745926

[Performance improvement of longwave infrared photodetector based on type-II InAs/GaSb superlattices using unipolar current blocking layers](#)

Appl. Phys. Lett. **96**, 231107 (2010); 10.1063/1.3446967



SHARE
your expertise in
simulation

TE11 cutoff frequency (fc): 4.868 Hz
Frequency: fc*1.2 Hz
Wavelength (λ): 0.5205 m
Flare angle: 17 °
Corrugation thickness: 0.105 m
Corrugation length: 0.155 m
Horn thickness: 0.5 m
Horn length: 4 m
Waveguide length: 1 m
Matching corrugation length: 0.25 m

WITH COMSOL APPS »

COMSOL

Input waveguide cross pol. ratio: 17.657 %
Output aperture cross pol. ratio: 3.025 %
 Target criterion: passed.

Evidence for a defect level above the conduction band edge of InAs/InAsSb type-II superlattices for applications in efficient infrared photodetectors

A. D. Prins,¹ M. K. Lewis,¹ Z. L. Bushell,¹ S. J. Sweeney,^{1,a)} S. Liu,² and Y.-H. Zhang²

¹Advanced Technology Institute and Department of Physics, University of Surrey, Guildford GU2 7XH, United Kingdom

²Center for Photonics Innovation and School of Electrical, Computer and Energy Engineering, Arizona State University, Tempe, Arizona 85287, USA

(Received 26 January 2015; accepted 20 April 2015; published online 29 April 2015)

We report pressure-dependent photoluminescence (PL) experiments under hydrostatic pressures up to 2.16 GPa on a mid-wave infrared InAs/InAs_{0.86}Sb_{0.14} type-II superlattice (T2SL) structure at different pump laser excitation powers and sample temperatures. The pressure coefficient of the T2SL transition was found to be $93 \pm 2 \text{ meV}\cdot\text{GPa}^{-1}$. The integrated PL intensity increases with pressure up to 1.9 GPa then quenches rapidly indicating a pressure induced level crossing with the conduction band states at ~ 2 GPa. Analysis of the PL intensity as a function of excitation power at 0, 0.42, 1.87, and 2.16 GPa shows a clear change in the dominant photo-generated carrier recombination mechanism from radiative to defect related. From these data, evidence for a defect level situated at $0.18 \pm 0.01 \text{ eV}$ above the conduction band edge of InAs at ambient pressure is presented. This assumes a pressure-dependent energy shift of $-11 \text{ meV}\cdot\text{GPa}^{-1}$ for the valence band edge and that the defect level is insensitive to pressure, both of which are supported by an Arrhenius activation energy analysis. © 2015 AIP Publishing LLC. [<http://dx.doi.org/10.1063/1.4919549>]

The III–V type-II superlattice (T2SL) is predicted to have a number of advantages over bulk HgCdTe infrared (IR) photodetectors including a decreased dependence of the bandgap on compositional non-uniformity, the ability to wavelength tune by changing layer thicknesses and alloy composition, the lower cost of III–V semiconductor substrates, a higher electron effective mass leading to smaller tunneling currents and band-engineered lower Auger recombination rates, and thus lower dark currents, as predicted theoretically.^{1,2} The widely studied InAs/GaInSb T2SLs have very short carrier lifetimes, on the order of 30 ns (Ref. 3) because the energy levels of intrinsic point defects in bulk GaSb are near the valence band edge or in the middle of the energy gap,⁴ leaving the trap states available for Shockley-Read-Hall (SRH) recombination. The other alternative approach, i.e., “Ga-free” InAs/InAsSb T2SLs⁵ has demonstrated a broad wavelength coverage from 4 μm to 12 μm ,^{6,7} and superior material performance, especially minority carrier lifetimes longer than 400 ns (Ref. 8) in the long-wave IR range and 10 μs in the mid-wave IR range⁹ as recently demonstrated. Such a dramatic improvement in minority carrier lifetime is believed to be due to the fact that in bulk InAs and As-rich InAsSb alloys the “stabilized Fermi level” is above the conduction band edge,⁴ rendering any mid-gap defect states inactive for SRH processes as demonstrated by relatively high photoluminescence (PL) efficiencies even when grown on highly mismatched GaAs substrates.¹⁰ Furthermore, Eastman and Freeouf¹¹ showed that empty surface states may exist within the bandgap of GaSb and above the conduction band edge of InAs. These observations have led us to investigate the intrinsic point defect energy levels in Ga-free T2SL structures to better understand why InAs/

InAsSb T2SLs have significantly longer minority carrier lifetimes.

In this paper, we set out to find experimental evidence to confirm that the defect energy states are above the conduction band edge of Ga-free T2SLs. Applying hydrostatic pressure to III–V semiconductors causes a strong and reversible change in their electronic band-structure¹² and is a perfect tool to investigate the fundamental properties of semiconductor systems and heterostructures as well as to probe recombination mechanisms in semiconductor devices.¹² Of most relevance to this study, the conduction band edge moves upwards in energy at a typical rate of $\approx 100 \text{ meV}\cdot\text{GPa}^{-1}$ for III–V semiconductors. This manifests itself very clearly through an increase in bandgap and, consequently, an increase in the optical transition energy with increasing pressure. In contrast, localized states such as defect energy states, are typically pressure insensitive owing to the fact that they are strongly localized and decoupled from the periodicity of the crystal.¹³ It is therefore possible to use high pressure to probe the interaction between the band edges and defect energy states, which, for example, may be seen through the quenching of PL or in an abrupt increase in the dark current of a photodetector due to increased non-radiative recombination. The experimental approach is similar to that used to find nitrogen complex levels above the conduction band edge of GaAs¹⁴ with high pressure, low temperature PL. Figure 1(a) shows a schematic representation of a Ga-free InAs/InAsSb T2SL band edge diagram and the suspected localized defect states at ambient pressure. The optical transition is shown as an arrow from the electron miniband above the conduction band edge of InAs to the hole miniband below the valence band edge of InAsSb. In Figure 1(a), the bandgap of InAs is 0.417 eV,¹⁵ for InAs_{0.86}Sb_{0.14} a value of 0.311 eV is determined based on parameters from Vurgaftman *et al.*¹⁵ and a bowing parameter of

^{a)} Author to whom correspondence should be addressed. Electronic mail: s.sweeney@surrey.ac.uk.

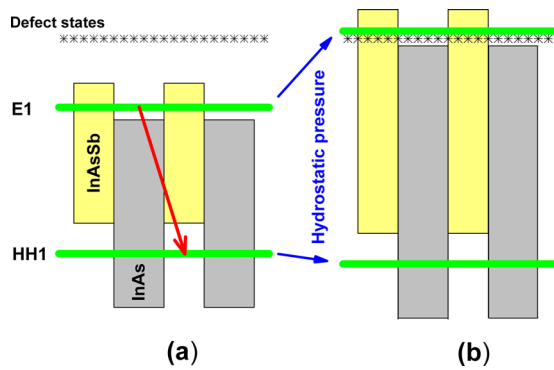


FIG. 1. (a) A schematic band edge diagram for a Ga-free InAs/InAsSb T2SL showing a defect state above the conduction band edge; (b) under hydrostatic pressure the effective bandgap energy increases, mainly due to an upward shift in the conduction band edge, while the defect states remain at the same energy. Quenching of the photoluminescence happens when the electron miniband edge moves close to the defect energy level.

0.65 eV.¹⁶ A fractional valence band offset, $Q_v = \Delta E_v / \Delta E_g$, of 1.75 ± 0.03 is used¹⁶ giving electron and hole well depths of 80 and 186 meV, respectively. The electron and hole minibands have confinement energies of 18 meV and 65 meV, respectively. The effect of applying pressure increases the effective bandgap of the T2SL, namely, the separation of the electron and the hole minibands. Most of the increase of the effective bandgap is due to the upward shift in energy of the conduction band edge and thus the electron miniband. It is anticipated that the PL intensity will decrease dramatically when the electron miniband moves above the defect energy level as shown in Figure 1(b), due to increased nonradiative recombination through the trap states of the defects.

The InAs/InAs_{0.86}Sb_{0.14} T2SL sample studied in this work was grown by molecular beam epitaxy on an n-type GaSb (100) substrate and contained a nominally undoped T2SL layer consisting of 48 periods of 8.1 nm InAs and 2.5 nm InAs_{0.86}Sb_{0.14} (see Figure 1(a)) with a lattice mismatch of 0.4%. The background doping density in this sample is estimated to be in the order of $1.0 \times 10^{16} \text{ cm}^{-3}$ n-type from low temperature Hall measurements. The growth details (sample B1761) and full optical and structural properties are reported elsewhere.^{7,17} PL experiments were performed at 10 K under pressure in a backscattering geometry in a clamp style sapphire ball cell (SBC).¹⁸ Methanol-ethanol (4:1) was used as the pressure transmitting media with pressure changes being carried out at room temperature before cooling down. PL was excited with a chopped 100 mW 1064 nm ND:YVO₄ laser with neutral density filters being placed in the beam to vary the pump power incident on the sample, generating excess carrier densities of more than a magnitude above the background doping density.^{3,9} PL measurements were carried out in a closed-cycle helium cryostat using a Triax 320 spectrometer with a liquid nitrogen cooled InSb detector and CaF₂ lenses. The pressure calibrant was an InGaAsP quantum well structure with a known linear pressure coefficient ($86 \text{ meV} \cdot \text{GPa}^{-1}$)¹⁹ which gave strong PL with peaks at 0.8145 eV and 0.8651 eV at room and low temperatures, respectively, but without any possible overlap with the T2SLs emission (0.3147 eV at 10 K). Both samples were thinned and loaded into the SBC after

confirming that the thinning process resulted in no change to their PL. The system spectral response (Triax grating, InSb detector, quartz cryostat window, two CaF₂ lenses, and a sapphire ball) was determined before and after the experimental runs using a Bentham traceable broadband light source to correct the measured PL spectra.

Four separate pressure runs were carried out with most of the data being taken with increasing pressure (several decreasing pressure cycle points were checked and gave good agreement). Figure 2(a) shows corrected PL spectra from one pressure run up to 2.16 GPa. Increased noise in the PL signal was seen over the range from 0.34 eV to 0.44 eV due to the absorption of the pressure medium over this wavelength range as shown in Figure 2(b). The interpolated transmission data²⁰ from liquid methanol and ethanol based on the 4:1 mixture ratio at 300 K (solid line) and the data from ethanol under pressure²¹ and frozen methanol spectra²² are used to estimate the shift and transmission behavior up to 2.16 GPa (dashed line). Based on this evidence it is clear that the transmission data changes with pressure, but whilst it was not possible for us to carry out a dynamic correction at each pressure and temperature we are able to show that the absorption should have little effect above 0.46 eV; this is confirmed by PL spectra from the InGaAsP pressure gauge.

The PL full width half maximum (FWHM) of the T2SL peak was 20 meV at an estimated excitation density of $13 \text{ W} \cdot \text{cm}^{-2}$ and decreased approximately linearly to around 15 meV at 1.5 GPa, above this it increased approximately linearly reaching 40 meV at 2.16 GPa. Figure 3(a) shows the collected peak emission energy data against pressure, which when fitted gives a pressure coefficient of $93 \pm 4 \text{ meV} \cdot \text{GPa}^{-1}$. This value is close to the quoted value of 96–108 $\text{meV} \cdot \text{GPa}^{-1}$ for InAs²³ and 128–155 $\text{meV} \cdot \text{GPa}^{-1}$ for InSb.²³ Calculations based on this structure using Nextnano software²⁴ and taking into account bandgap and effective mass changes, show that the confinement energy of the electron states changes by as little as 1 meV up to 2.16 GPa. The change in strain is negligible as the two constituent layers of the T2SL have similar elastic constants. The initial electron confinement is calculated as 18 meV in the superlattice well of depths of 80 meV.

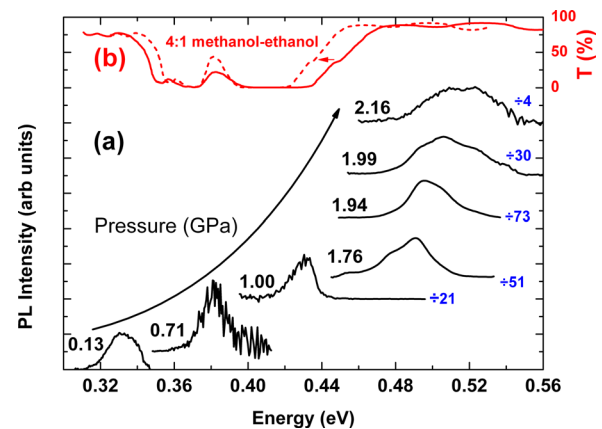


FIG. 2. (a) Photoluminescence spectra acquired from one run at different hydrostatic pressures up to 2.16 GPa. (b) On the same energy axis the optical transmission “T” (from 0% to 100%) of the methanol-ethanol pressure transmitting media calculated from literature data at 0 GPa (solid line), the arrow indicates the shift to the estimated transmission at 2.16 GPa (dashed line).

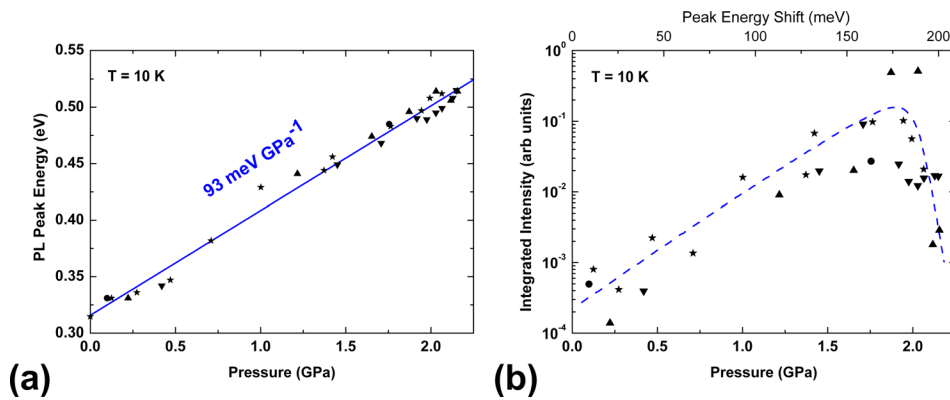


FIG. 3. (a) A linear fit of the photoluminescence peak energy data obtained for the T2SL sample from the four pressure runs indicated using four different symbols. (b) The integrated photoluminescence intensity of the T2SL sample plotted as a function of pressure and also peak energy shift from ambient pressure on the top axis. The dashed line is drawn as a guide to the eye.

This well depth deepens slightly with pressure but importantly the electron miniband is expected to shift at the same rate as the InAs layer.

Figure 3(b) shows all of the integrated PL intensity data corrected for the system response and optical collection efficiency from the four pressure runs as a function of pressure and peak energy shift. An energy level crossover between a defect energy level (or another conduction band minima) and a conduction band edge state is normally accompanied by a strong decrease in the integrated PL intensity as seen in InAs/GaAs quantum dots undergoing a Γ -X crossover²⁵ and may also give rise to new radiative peaks moving with different or negative pressure coefficients.^{14,25} With increasing pressure, and after a comparatively large initial increase of over two orders of magnitude,²⁵ Figure 3(b) shows such a decrease in PL intensity but we report no change in the pressure coefficient of the PL peak energy associated with this quenching nor any new radiative peaks above the crossover pressure. All these characteristics are expected in the case of a crossover with a non-radiative defect level. PL was not observed above the pressures shown in Figure 3(b) as the defect energy levels move below the conduction band edge and into the InAs bandgap becoming SRH recombination centers.

A careful comparison of the energy and intensity data shown in Figure 3(b) and those reported by Itskevich *et al.*²⁵ and elsewhere indicates a crossover at 2 GPa. This corresponds to a PL energy shift of 0.186 eV (onset at 1.92 GPa with the true crossover close to 2 GPa, giving 1.96 ± 0.04 GPa or an energy shift of $\sim 0.18 \pm 0.01$ eV). According to Daunov *et al.*,²⁶

the ratio of the pressure coefficients of the conduction and valence band edges for many III-V semiconductors (including InSb) are equal to ~ 7 . For our structure this would mean that $82 \text{ meV} \cdot \text{GPa}^{-1}$ of the determined pressure coefficient of our sample would go into the conduction band edge with the valence band edge moving down at a rate of $-11 \text{ meV} \cdot \text{GPa}^{-1}$. Assuming that the defect energy level does not move with pressure, as shown in Figure 1, using the above conduction band edge shift over 2 GPa and adding the 17 meV confinement energy at 2 GPa leads to a determined defect level ~ 0.18 eV above the InAs conduction band edge at ambient pressure. More details about this assignment will be discussed further below.

The PL intensity data as a function of laser excitation power and temperature under pressure are plotted in Figure 4 and examined to confirm that the PL quenching at 2 GPa is indeed due to a change from a radiative dominant recombination process to a non-radiative dominant recombination mechanism. Figure 4(a) shows the excitation power dependence of the T2SL integrated PL intensity data at 0, 0.42, 1.87, and 2.16 GPa at 10 K.

The observed PL intensity as a function of excitation power density is easily described by a power law with a fitted power exponent at 0 GPa of 0.91, close to 1, which, for an undoped sample, such as that discussed here, clearly indicates a dominant radiative recombination process.^{27,28} A similar gradient is seen at 0.42 GPa, confirming that the recombination is radiative in nature and that mid gap SRH recombination is negligible at low pressure. At 1.87 GPa (the onset of the high pressure PL intensity decline), the measured gradient

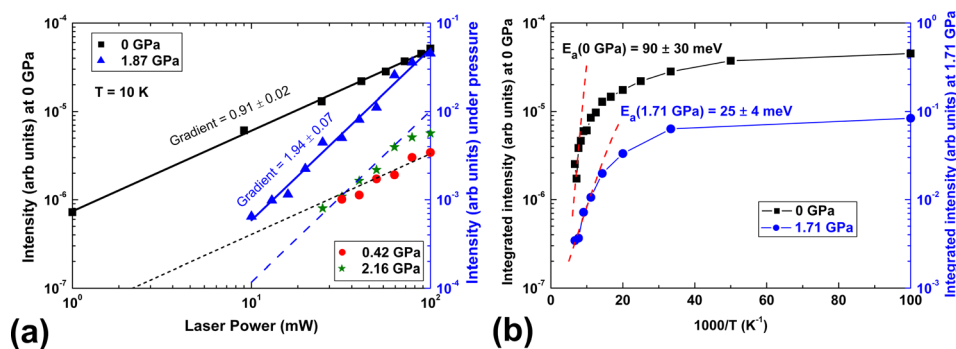


FIG. 4. (a) Power dependent PL measurements taken at 0 GPa (intensity axis on left), and 0.42, 1.87, and 2.16 GPa (intensity axis on right). Solid lines show linear fits of the PL intensity at 0 and 1.87 GPa. Dotted and broken lines are the same fits offset as a guide to the eye at 0.42 GPa and 2.16 GPa, respectively. (b) Arrhenius plots of data at 0 GPa (left intensity axis) and 1.71 GPa (right intensity axis). Dashed lines in the high temperature range are marked with the determined activation energy (E_a) in meV.

is 1.94. This value is close to 2, which indicates a dominant non-radiative, defect-related recombination path is now involved. Finally, at 2.16 GPa a gradient close to 1.94 is seen but with possible evidence of saturation at the highest laser power. All the data in Figure 4(a) confirm our expectation that the PL quenching at 2 GPa is the result of a transition from dominant radiative recombination to dominant non-radiative recombination.

Assuming that the non-radiative recombination can also be thermally activated we studied the integrated PL intensity quenching from 10 K to 150 K at 0 GPa and 1.71 GPa and the measured results are shown in Figure 4(b). At high pressure and over this low temperature range, it should be noted that the pressure medium remains solid and the pressure is constant within the SBC.

From Figure 4(b), it can be seen that the higher temperature behavior of each data set follows an exponential dependence,²⁹ from which activation energies have been calculated. The 0 GPa data gives an activation energy of 90 ± 30 meV, but at 1.71 GPa a much lower value of 25 ± 4 meV is obtained. Our measured activation energy of 90 meV at 0 GPa may be related to the depth of the electron well (80 meV). At 1.71 GPa, it is 0.29 GPa from our determined crossover pressure (2 GPa) and using our conduction band edge pressure coefficient of $82 \text{ meV} \cdot \text{GPa}^{-1}$ we estimate that the energy level associated with the quenching is ~ 24 meV away. This data confirms our assumptions of the pressure-dependent energy shifts of the valence band and conduction band edges. It also points to the fact that the defect level is indeed not moving with pressure, as if it were then the activation energy obtained at 1.71 GPa would not be consistent with our results as the rate at which the confined electron state approached the defect would depend on both pressure coefficients. We note here that the nature and exact identification of these defect states is outside of the scope of this present work, but will be investigated in the future studies.

In summary, we have performed pressure-dependent PL measurements on an InAs/InAs_{0.86}Sb_{0.14} T2SL structure. By fitting the measured peak energy shift and observing a quenching of the PL intensity, we have determined a crossover pressure at which we believe the T2SL electron confined state reaches that of a defect level in the superlattice. This change in nature from a radiative to non-radiative recombination mechanism with pressure is confirmed from power dependent PL measurements. We also examine the thermal activation energies at ambient pressure and close to the crossover pressure which support and are consistent with the determined values for the pressure coefficients of the valence and conduction band edges of the structure and the defect level. As a result, these experiments provide strong evidence that the defect level is approximately 180 meV above the conduction band edge of InAs. Consequently, these findings explain why Ga-free T2SL structures have much longer minority carrier lifetimes, a highly desirable advantage for both mid-wave and long-wave IR photodetector applications.

The authors thank Steve Craig and Chris Buxey for their technical assistance with this work and Zhiyuan Lin for

valuable input and discussions. The authors gratefully acknowledge financial support from EPSRC (UK) Project Nos. EP/H005587/1 and EP/H050787/1 and for a vacation studentship for Z.B., the South-East England Physics Network (SEPnet) for a studentship for M.K.L., and ARO MURI programs with Contract No. W911NF-10-1-0524 and another ARO research program with Contract No. W911NF-14-1-0388.

¹D. L. Smith and C. Mailhot, *J. Appl. Phys.* **62**, 2545 (1987).

²C. H. Grein, M. E. Flatte, and H. Ehrenreich, in *Proceedings of 3rd International Symposium on LWIR Detectors and Arrays: Physics and Applications III* (1995), p. 211.

³B. C. Connelly, G. D. Metcalfe, H. Shen, and M. Wraback, *Appl. Phys. Lett.* **97**, 251117 (2010).

⁴W. Walukiewicz, *Mat. Res. Soc. Symp. Proc.* **148**, 137 (1989); *Phys. Rev.* **37**, 4760 (1988).

⁵Y.-H. Zhang, *Appl. Phys. Lett.* **66**, 118 (1995); A. Y. Lew, E. T. Yu, and Y.-H. Zhang, *J. Vac. Sci. Technol.*, **B 14**, 2940 (1996).

⁶D. Lackner, O. J. Pitts, M. Steger, A. Yang, M. L. W. Thewalt, and S. P. Watkins, *Appl. Phys. Lett.* **95**, 081906 (2009).

⁷O. O. Cellek, H. Li, X.-M. Shen, Z. Lin, E. H. Steenbergen, D. Ding, S. Liu, Q. Zhang, H. S. Kim, J. Fan, M. J. DiNezza, W. H. G. Dettlaff, P. T. Webster, Z. He, J.-J. Li, S. R. Johnson, D. J. Smith, and Y.-H. Zhang, *Proc. SPIE* **8353**, 83533F (2012).

⁸E. H. Steenbergen, B. C. Connelly, G. D. Metcalfe, H. Shen, M. Wraback, D. Lubyshev, Y. Qiu, J. M. Fastenau, A. W. K. Liu, S. Elhamri, O. O. Cellek, and Y.-H. Zhang, *Appl. Phys. Lett.* **99**, 251110 (2011).

⁹Y. Aytac, B. V. Olson, J. K. Kim, E. A. Shaner, S. D. Hawkins, J. F. Klem, M. E. Flatté, and T. F. Boggess, *Appl. Phys. Lett.* **105**, 022107 (2014).

¹⁰P. Tang, M. J. Pullin, S. J. Chung, C. C. Phillips, R. A. Stradling, A. G. Norman, Y. B. Li, and L. Hart, *Semicond. Sci. Technol.* **10**, 1177 (1995).

¹¹D. E. Eastman and J. L. Freeouf, *Phys. Rev. Lett.* **34**, 1624 (1975).

¹²A. Prins, A. Adams, and S. Sweeney, "Pressure studies," in *Semiconductor Research Experimental Techniques*, edited by A. Patane and N. Balkan (Springer, Heidelberg, Germany, 2012), Vol. 150, Chap. 6.

¹³R.-D. Hong, D. W. Jenkins, S. Y. Ren, and J. D. Dow, *Phys. Rev. B* **38**, 12549 (1988).

¹⁴X. Liu, M.-E. Pistol, L. Samuelson, S. Schwetlick, and W. Seifert, *Appl. Phys. Lett.* **56**, 1451 (1990).

¹⁵I. Vurgaftman, J. R. Meyer, and L. R. Ram-Mohan, *J. Appl. Phys.* **89**, 5815 (2001).

¹⁶E. H. Steenbergen, O. O. Cellek, D. Lubyshev, Y. Qiu, J. M. Fastenau, A. W. K. Liu, and Y.-H. Zhang, *Proc. SPIE* **8268**, 82680K (2012).

¹⁷H. Li, S. Liu, O. O. Cellek, D. Ding, X.-M. Shen, E. H. Steenbergen, J. Fan, Z. Lin, Z.-Y. He, Q. Zhang, P. T. Webster, S. R. Johnson, L. Ouyang, D. J. Smith, and Y.-H. Zhang, *J. Cryst. Growth* **378**, 145–149 (2013).

¹⁸W. B. Daniels, M. Lipp, D. Strachan, D. Winters, and Z.-H. Yu, in *Proceedings of the XIII AIRAPT International Conference on High Pressure Science and Technology*, edited by A. K. Singh (Oxford & IBH Publishing Co., New Delhi, 1992), pp. 809–811.

¹⁹A. F. Phillips, S. J. Sweeney, A. R. Adams, and P. J. A. Thijs, *IEEE J. Sel. Top. Quantum Electron.* **5**, 401 (1999).

²⁰E. K. Plyler, *J. Res. Natl. Bur. Stand.* **48**, 281 (1952).

²¹A. Anderson, J. Benson, and W. Smith, *Spectrosc. Lett.* **31**, 369 (1998).

²²M. Falk and E. Whalley, *J. Chem. Phys.* **34**, 1554 (1961).

²³P. E. Van Camp, V. E. Van Doren, and J. T. Devreese, *Phys. Rev. B* **41**, 1598 (1990).

²⁴See <http://www.nextnano.de> for Nextnano Semiconductor Software Solutions.

²⁵I. E. Itskevich, S. G. Lyapin, I. A. Troyan, P. C. Klipstein, L. Eaves, P. C. Main, and M. Henini, *Phys. Rev. B* **58**, R4250 (1998).

²⁶M. I. Daunov, I. K. Kamilov, S. F. Gabibov, and A. B. Magomedov, *Phys. Status Solidi B* **235**(2), 297–301 (2003).

²⁷W. Feng, Y. Wang, J. Wang, W. K. Ge, Q. Huang, and J. M. Zhou, *Appl. Phys. Lett.* **72**, 1463 (1998).

²⁸X. Chen, Y. Zhou, L. Zhu, Z. Qi, Q. Xu, Z. Xu, S. Guo, J. Chen, L. He, and J. Shao, *Jpn. J. Appl. Phys., Part 1* **53**, 082201 (2014).

²⁹J. L. Pankove, *Optical Processes in Semiconductors* (Dover, New York, 1971), pp. 165–166.